Available online at www.sciencedirect.com
SCIENCE DIRECT®
Journal of Solid State Chemistry 177 (2004) 834–838
JOURNAL OF SOLID STATE CHEMISTRY
http://elsevier.com/locate/jssc

Studies of microstructure and ruthenium valence in the ruthenocuprates $Pb_2RuSr_2Cu_2O_8Cl$ and (Ru, M)$Sr_2GdCu_2O_8$ (M = Sn, Nb)

A.C. Mclaughlin,[a,b] J.P. Attfield,[a,b,*] R.S. Liu,[c] L.-Y. Jang,[d] and W.Z. Zhou[e]

[a] *Department of Chemistry, University of Cambridge, Lensfield Road, Cambridge CB2 1EW, UK*
[b] *Department of Physics, Interdisciplinary Research Centre in Superconductivity, University of Cambridge, Madingley Road, Cambridge CB3 0HE, UK*
[c] *Department of Chemistry, National Taiwan University, Taipei 106, Taiwan, ROC*
[d] *National Synchrotron Radiation Research Center (NSRRC), Hsinchu 300, Taiwan, ROC*
[e] *School of Chemistry, University of St Andrews, St. Andrews KY16 9ST, UK*

Received 15 July 2003; received in revised form 11 September 2003; accepted 17 September 2003

Abstract

Ruthenocuprate microstructures and Ru valences have been studied. Electron microscopy reveals short-range order of the RuO_6 octahedra rotations into a $\sqrt{2}a \times \sqrt{2}a \times c$ supercell in $Pb_2RuSr_2Cu_2O_8Cl$. However, reanalysis of neutron diffraction data gives no significant difference between the populations of the rotation states, showing that the coherence length is very short (< 100 Å). The Ru valence estimated from the XANES spectrum of $Pb_2RuSr_2Cu_2O_8Cl$ is ~5, in keeping with the physical properties of this material which show that there is essentially no Ru–Cu charge transfer. The Ru valence in doped $Ru_{1-x}M_xSr_2GdCu_2O_8$ (M = Sn, Nb) is ~4.8 in all samples, verifying a previous rigid band analysis of the charge distribution in these materials.

Keywords: Ruthenocuprate; Superconductivity; Magnetism; HREM; XANES

1. Introduction

Since the discovery of coexisting superconductivity and weak ferromagnetism in the ruthenocuprates, the physical and magnetic properties of the materials $RuSr_2GdCu_2O_8$ and $RE_{2-x}Ce_xRuSr_2Cu_2O_{10-\delta}$ have been studied extensively [1–28]. The superconductivity originates in the CuO_2 planes with $T_c = 37$ K for the former material, and the weak ferromagnetism is associated with the ruthenate layers [3–5]. G-type antiferromagnetic order within the RuO_2 planes has been observed in neutron scattering experiments on $RuSr_2GdCu_2O_8$ below $T_M = 134$ K [12]. Variable field neutron diffraction studies of this material showed that the Ru spins cant into a ferromagnetic arrangement upon the application of a magnetic field and at 7 T the Ru spins are fully ferromagnetic. It is thought that the weak ferromagnetism arises via a canting of the Ru spins in $RuSr_2GdCu_2O_8$. This occurs due to the antisymmetric Dzyaloshinsky–Moriya interaction between neighbouring Ru moments, [29,30] which is non-zero due to the tilts and rotations of the RuO_6 octahedra observed in synchrotron X-ray and neutron diffraction studies [9–11]. Recent neutron and synchrotron X-ray powder diffraction studies have shown that rotations and tilts of the RuO_6 octahedra also occur in $Gd_{1.3}Ce_{0.7}RuSr_2Cu_2O_{10}$ [27,28] and it is thought that a similar magnetic mechanism occurs although there has been no evidence of this from neutron diffraction studies as yet.

A new ruthenocuprate $Pb_2RuSr_2Cu_2O_8Cl$ has recently been synthesized; this material is of similar structure to $RuSr_2GdCu_2O_8$ (Fig. 1(a)) but diamagnetic Pb_2Cl layers replace Gd [31,32] (Fig. 1(b)). Field dependent magnetism is observed in the ruthenate layers of $Pb_2RuSr_2Cu_2O_8Cl$; G type antiferromagnetism is observed below $T_M = 117$ K but above $H = 0.5$ T the Ru

*Corresponding author. Department of Chemistry, University of Cambridge, Lensfield Road, Cambridge CB2 1EW, UK. Fax: +44-1223-336362.
E-mail address: jpa14@cam.ac.uk (J.P. Attfield).

0022-4596/$ - see front matter © 2003 Elsevier Inc. All rights reserved.
doi:10.1016/j.jssc.2003.09.016

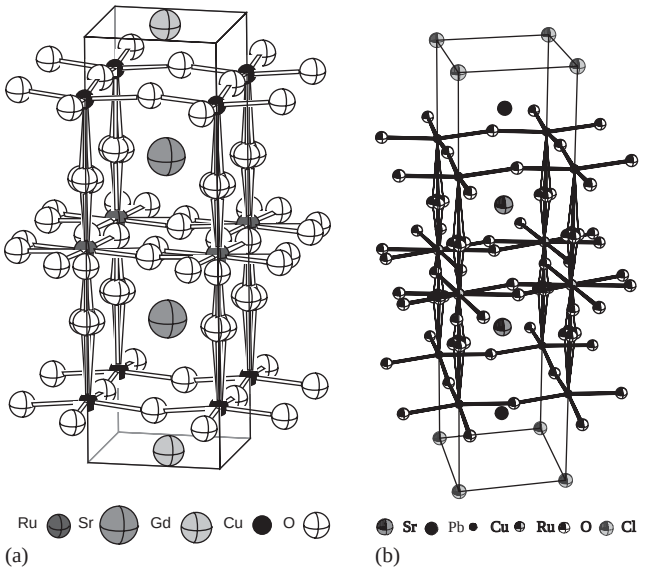

Fig. 1. Average crystal structures of (a) $RuSr_2GdCu_2O_8$ and (b) $Pb_2RuSr_2Cu_2O_8Cl$ showing the tilts and rotations of the RuO_6 octahedra.

spins cant into a ferromagnetic arrangement yielding a saturated Ru moment of 0.5–0.8 μ_B. Despite the similarity of both crystal and magnetic structures to $RuSr_2GdCu_2O_8$, $Pb_2RuSr_2Cu_2O_8Cl$ is not superconducting and it is thought that the RuO_2 planes contain Ru^{5+} with little or no electron doping to the Ru^{4+} state.

In order to investigate the charge distribution further we have performed X-ray absorption near-edge structure (XANES) spectroscopy to determine the Ru valence state. For comparison, we have also performed XANES studies on two sets of doped samples $Ru_{1-x}M_xSr_2GdCu_2O_8$ (M = Nb, Sn) [33,34] to observe any change in Ru valence upon doping. The microstructures of the ruthenocuprate materials have also been of interest, and we report here high-resolution transmission electron microscopy (HRTEM) studies and selected area electron diffraction (SAED) experiments on $Pb_2RuSr_2Cu_2O_8Cl$.

2. Experimental

The preparation of the $Pb_2RuSr_2Cu_2O_8Cl$ sample has been described previously [31,32]. This phase is very difficult to prepare in a pure form, and previous phase analysis has shown that the sample contains 73% (by mass) $Pb_2RuSr_2Cu_2O_8Cl$, 8% CuO and 19% $SrRuO_3$, estimated by Rietveld fitting of time-of-flight powder neutron diffraction data. Preparation of ceramic samples of $Ru_{1-x}M_xSr_2GdCu_2O_8$ (M = Sn: $x = 0$, 0.025, 0.05, 0.075; M = Nb: $x = 0$, 0.05, 0.1, 0.15, 0.2) has been reported previously [33,34]. All samples are >98% pure.

HRTEM studies of $Pb_2RuSr_2Cu_2O_8Cl$ were performed on a JEOL JEM-2010 electron microscope operating at 200 kV. The lens parameter Cs is 0.5 mm and the corresponding point resolution is about 0.19 nm. The images were recorded by using a Gatan 794 CCD camera with original magnification of 800,000 × and the SAED patterns were recorded on film.

XANES measurements were performed on beamline BL15B at NSRRC in Hsinchu, Taiwan using a Si(111) double-crystal monochromator. The Ru L_{III}-edge X-ray absorption spectra of the polycrystalline samples were recorded in the fluorescence mode using a modified Lytle detector [21,25]. Both the L_{II} and L_{III} edges of Mo and Pd metallic foils were used to calibrate the photon energies and the AUTOBK code was used for background subtraction [35]. The fitting procedures have been described elsewhere [21,25].

3. Results

3.1. $Pb_2RuSr_2Cu_2O_8Cl$ microstructure

A typical HRTEM image of $Pb_2RuSr_2Cu_2O_8Cl$ is shown in Fig. 2. This confirms the layer stacking observed in the crystal structure with an 8-layer repeat sequence along the c-axis. However, many extended defects are also observed; the region in Fig. 2 shows a stacking fault (black arrow) and a dislocation defect (white arrow).

All of the main diffraction spots in the SAED pattern of $Pb_2RuSr_2Cu_2O_8Cl$ could be indexed by the basic tetragonal cell ($P4/mmm$, $a = 3.87$ Å and $c = 15.37$ Å) as previously observed from neutron diffraction studies

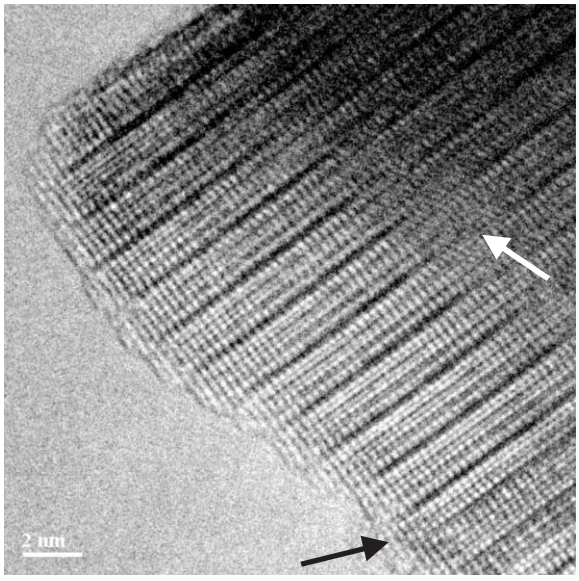

Fig. 2. HRTEM image of a region of $Pb_2RuSr_2Cu_2O_8Cl$ showing layered defects as indicated by arrows.

on the same sample [31,32]. However additional weak $(h/2\,k/2\,0)$ spots in the [001] zone axis indicate the formation of a $\sqrt{2}a \times \sqrt{2}a \times c$ superstructure (Fig. 3). This superstructure has also been observed in SAED patterns of $RuSr_2GdCu_2O_8$ [9]. It results from rotations of the RuO_6 octahedra around c due to the bond length mismatch between the RuO_2 and CuO_2 layers. The rotations of the RuO_6 octahedra would give rise to a $\sqrt{2}a \times \sqrt{2}a \times c$ superstructure if long-range ordered, however only partial ordering has been observed from HRTEM and neutron diffraction studies of $RuSr_2GdCu_2O_8$ [9,11].

Rotations and tilts of the RuO_6 octahedra were observed in the previous neutron refinement of the $Pb_2RuSr_2Cu_2O_8Cl$ [31,32] structure in the basic $P4/mmm$ $a \times a \times c$ tetragonal cell. The neutron refinement has been repeated using the approach reported to model the partial ordering of the RuO_6 octahedra in $RuSr_2GdCu_2O_8$ [11]. The structure is refined in the tetragonal, $P4/mbm$ symmetry, $\sqrt{2}a \times \sqrt{2}a \times c$ supercell, and a second oxygen site within the RuO_2 layer, O(3)′, which represents the minority fraction of RuO_6 octahedra rotated in the opposite sense, is introduced. Using the GSAS program [36] to fit the principal and impurity phase structures gave an excellent Rietveld fit [37] to the 295 K data. The co-ordinates are shown in Table 1. Unconstrained refinement of the fractional occupancies of O(3) and O(3)′ gave 0.47(3) and 0.51(3), respectively. This demonstrates that the coherence length for the octahedral rotations is very short (<100 Å) in $Pb_2RuSr_2Cu_2O_8Cl$, and is consistent with the lack of any superstructure peaks in the neutron diffraction data.

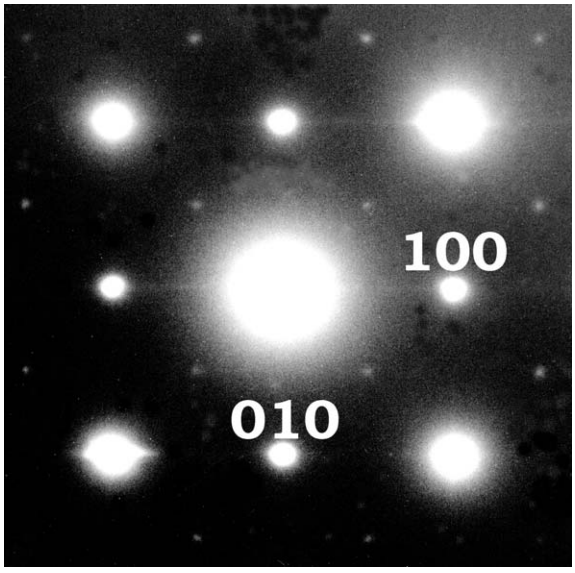

Fig. 3. SAED pattern from $Pb_2RuSr_2Cu_2O_8Cl$ viewed down the [001] direction. The main diffraction spots are indexed by the $P4/mmm$ tetragonal cell with $a = 3.87$ and $c = 15.37$ Å. The additional weak spots evidence the $\sqrt{2}a \times \sqrt{2}a \times c$ superstructure.

3.2. Ru valences

Recent X-ray Absorption Near Edge Spectroscopy (XANES) studies on $RE_{2-x}Ce_xRuSr_2Cu_2O_{10}$ and $RuSr_2GdCu_2O_8$ have indicated that the average Ru valence state can vary significantly, with values of 4.6 [21] for $RuSr_2RECu_2O_8$ and between 5.0 and 4.95 [25] for $RE_{2-x}Ce_xRuSr_2Cu_2O_{10}$ being determined. We have used this technique in an attempt to determine the Ru valence of the ruthenocuprates $Pb_2RuSr_2Cu_2O_8Cl$ and $Ru_{1-x}M_xSr_2Cu_2O_8$ (M = Nb, Sn). The L_{III}-edge XANES spectra of $Pb_2RuSr_2Cu_2O_8Cl$ and $Ru_{0.95}M_{0.05}Sr_2Cu_2O_8$ (M = Nb, Sn) are shown in Figs. 4(a) and (b), respectively. The reference spectra of Sr_2GdRuO_6 (Ru^{5+}) and Sr_2RuO_4 (Ru^{4+}) are also shown. Ru is in octahedral co-ordination in each of these materials and hence the crystal field of O_h symmetry leads to a splitting of the 4d states into t_{2g} and e_g levels separated by $\Delta(= 10\,Dq)$. The lower energy peak corresponds to a $2p \rightarrow t_{2g}$ transition and the higher

Table 1
Refined cell parameters, agreement factors and atomic parameters for $Pb_2RuSr_2Cu_2O_8Cl$ at 295 K in the $P4/mbm$ space group

	a (Å)	c (Å)	Volume (Å^3)	R_{WP} (%)	R_p (%)	χ^2
	5.4671(2)	15.3674(9)	459.31(5)	2.41	2.28	10.0
Atom	Site	x	y	z	U_{iso} (Å^2)	Occupancy
Pb	4(f)	0.5	0	0.3759(2)	0.0067(5)	1
Ru	2(a)	0	0	0	0.0046(8)	1
Sr	4(f)	0.5	0	0.1436(2)	0.0053(7)	1
Cu	4(e)	0	0	0.2704(2)	0.0008(5)	1
O(1)	4(e)	0	0	0.1255(3)	0.0092(8)	1
O(2)	8(k)	0.2370(7)	0.2630(7)	0.2807(2)	0.0044(7)	1
O(3)	4(g)	0.1902(7)	0.6902(7)	0	0.012(1)	0.47(3)
O(3)′	4(g)	0.6902(7)	0.1902(7)	0	0.013(1)	0.51(3)
Cl	2(b)	0	0	0.5	0.036(1)	1

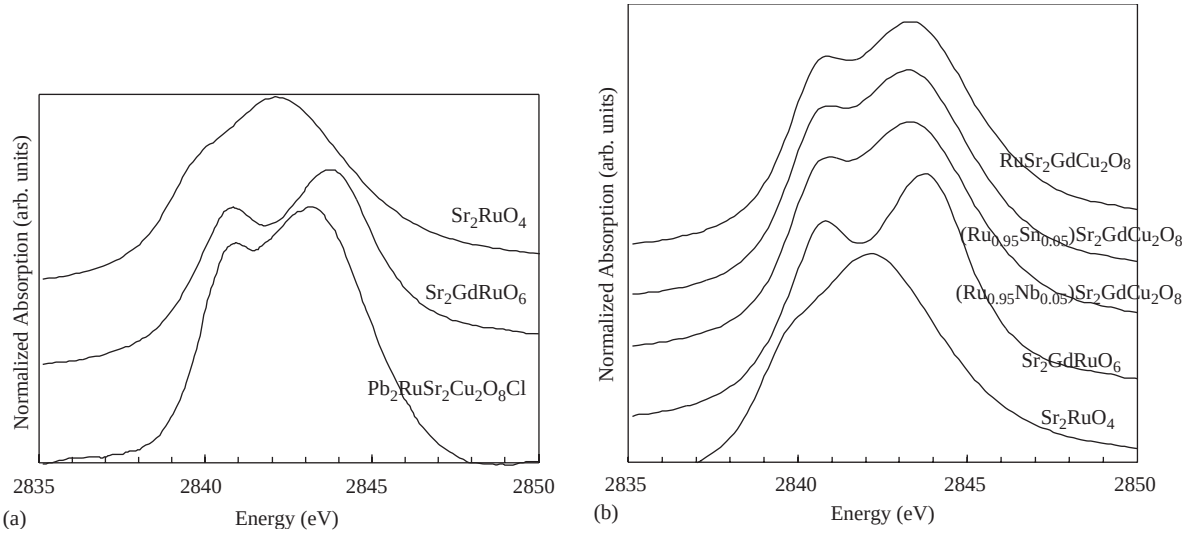

Fig. 4. Ru L_{III}-edge X-ray absorption near edge structure for (a) $Pb_2RuSr_2Cu_2O_8Cl$ and (b) $RuSr_2GdCu_2O_8$, $Ru_{0.95}Nb_{0.05}Sr_2GdCu_2O_8$ and $Ru_{0.95}Sn_{0.05}Sr_2GdCu_2O_8$. Also shown are spectra for the reference samples Sr_2GdRuO_6 and Sr_2RuO_4.

energy peak corresponds to a $2p \rightarrow e_g$ transition [38]. The average Ru valence in each sample was obtained by fitting a linear combination of the Sr_2RuO_4 and Sr_2GdRuO_6 spectra to the XANES spectra of $Pb_2RuSr_2Cu_2O_8Cl$ and $Ru_{1-x}M_xSr_2Cu_2O_8$ (M = Nb, Sn). This method was previously used to determine the Ru valence of $RuSr_2RECu_2O_8$ and $RE_{2-x}Ce_xRuSr_2Cu_2O_{10}$ [21,25].

The XANES spectra of $Pb_2RuSr_2Cu_2O_8Cl$ (Fig. 4(a)) and $Ru_{1-x}M_xSr_2GdCu_2O_8$ (M = Nb, Sn) (Fig. 4(b)) are very similar and the average Ru valence estimated by the above method is 4.8 for all the samples. The separation of the two peaks gives the crystal field splitting as $\Delta = 2.2\,\text{eV}$ ($18000\,\text{cm}^{-1}$) for $Pb_2RuSr_2Cu_2O_8Cl$ and $\Delta = 2.4\,\text{eV}(19000\,\text{cm}^{-1})$ for $Ru_{1-x}M_xSr_2GdCu_2O_8$.

4. Discussion

The microscopy study of $Pb_2RuSr_2Cu_2O_8Cl$ demonstrates similar microstructural features to those found in the other (1212 and 2122) ruthenocuprate families. This was first observed in HRTEM images of $RuSr_2GdCu_2O_8$ that evidenced anti-phase boundaries at which the sense of rotation of the RuO_6 octahedra around c is reversed but the rest of the structure is unaffected, dividing the structure into subdomains of 50–200 Å [9]. This was subsequently modelled from neutron diffraction data on an isotopically enriched sample of $RuSr_2GdCu_2O_8$ using the $P4/mbm$ supercell [11]. For this sample, neutron superstructure peaks were observed and the RuO_2-plane majority and minority oxygen site occupancies refined to 0.70(1) and 0.27(1), respectively. However, the analogous refinement of the $Pb_2RuSr_2Cu_2O_8Cl$ reported here (Table 1) gives O(3) and O(3)′ site occupancies that do not differ significantly, although the superstructure is observed by SAED (Fig. 3).

It has been suggested that the fractional population of the two domains in $RuSr_2GdCu_2O_8$ depends upon the annealing of the sample [9,11]. Upon cooling, domains with a particular sense of rotation nucleate and grow, and a well-annealed sample may approach a single domain in each crystallite although full ordering has not yet been observed. The $Pb_2RuSr_2Cu_2O_8Cl$ sample was prepared by firing the ceramic pellet for a relatively short time (10 h) at 700°C followed by quenching, to minimize the formation of secondary phases. This evidently does not allow long-range coherence of the RuO_6 rotations to develop, and in comparison to $RuSr_2GdCu_2O_8$, the domains are evidently small (< 100 Å) in extent.

The intrinsic doping of the copper oxide planes that leads to superconductivity in $RuSr_2GdCu_2O_8$ results from Ru and Cu band overlap, which is represented by the formal oxidation states in the formula $Ru^{5-2p_0^+}Sr_2GdCu_2^{2+p_0^+}O_8$. The intrinsic hole doping p_0 is estimated to be 0.08. This was supported by substituting Ru in $RuSr_2GdCu_2O_8$ with fixed-valent cations Nb^{5+} and Sn^{4+} on the Ru site. The results were analyzed assuming a rigid band structure, i.e. that p_0 is fixed, so that the doping effects at the CuO_2 planes comes from the difference between the charge on Ru and M^{q+} ($=Nb^{5+}$ or Sn^{4+}) according to the formula $(Ru_{1-x}^{5-2p_0^+}M_x^{q^+})Sr_2GdCu_2^{2+p_0+x(p_0+5-q)/2}O_8$. Hence, the Ru valence should not change with substitution. The present XANES results (Fig. 4(b)) provide an important corroboration of this, as no shift in the Ru edge is observed within the $Ru_{1-x}M_xSr_2GdCu_2O_8$ solid solutions. This is in stark contrast to XANES results on $RuSr_2(Gd_{1-x}Dy_x)Cu_2O_8$ and $Ru(Sr_{2-x}Ba_x)GdCu_2O_8$,

where the Ru valence was found to decrease with Dy doping and increase with Ba doping [21]. In these materials, the intrinsic hole transfer p_0 is changed by the lattice effects resulting from the size of the substituted cation. Dy^{3+} is smaller than Gd^{3+} which tends to decrease the Cu–O distances in the adjacent CuO_2 planes, resulting in an increase in p_0 and so a decrease in the Ru valence. Replacing Sr^{2+} by the larger Ba^{2+} tends to expand the lattice by reducing the hole concentration in the CuO_2 planes, so the Ru valence increases.

The Ru valence of 4.8 in the $Pb_2RuSr_2Cu_2O_8Cl$ sample measured by XANES is a weighted average of the values for $Pb_2RuSr_2Cu_2O_8Cl$ and the $SrRuO_3$ impurity. The latter material may itself be doped, most probably by Pb^{4+} substituting for Ru^{4+}, as evidenced previously [32]. Nevertheless, the Ru valence in this phase will be close to $+4$, so the average sample valence of 4.8 shows that Ru in $Pb_2RuSr_2Cu_2O_8Cl$ is very close to Ru^{5+}. This is consistent with the physical properties [32] which showed that there is essentially no Ru–Cu charge transfer in this material.

Acknowledgments

We thank EPSRC for the provision of research grant GR/M59976 and a studentship for ACM.

References

[1] L. Bauernfeind, W. Widder, H.F. Braun, Physica C 254 (1995) 151.
[2] L. Bauernfiend, W. Widder, H.F. Braun, J. Low Temp. Phys. 105 (1996) 1605.
[3] I. Felner, U. Asaf, Y. Lavi, O. Milio, Phys. Rev. B 55 (1997) 3374.
[4] J.L. Tallon, C. Bernhard, M. Bowden, P. Gilberd, T. Stoto, D. Pringle, IEEE Trans. Appl. Supercond. 9 (1999) 1696.
[5] C. Bernhard, J.L. Tallon, C. Niedermayer, T. Blasius, A. Golnik, E. Brucher, R.K. Kremer, D.R. Noakes, C.E. Stronach, E.J. Ansaldo, Phys. Rev. B 59 (1999) 14099.
[6] K.B. Tang, Y.T. Qian, L. Yang, Y.D. Zhao, Y.H. Zhang, Physica C 282–287 (1997) 947.
[7] I. Felner, U. Asaf, S. Reich, Y. Tsabba, Physica C 163 (1999) 311.
[8] J.L. Tallon, J.W. Loram, G.V.M. Williams, C. Bernhard, Phys. Rev. B 61 (2000) 6471.
[9] A.C. Mclaughlin, W. Zhou, J.P. Attfield, A.N. Fitch, J.L. Tallon, Phys. Rev. B 60 (1999) 7512.
[10] A.C. Mclaughlin, J.P. Attfield, J.L. Tallon, Int. J. Inorg. Mater. 2 (2000) 95.
[11] O. Chmaissem, J.D. Jorgensen, H. Shaked, P. Dollar, J.L. Tallon, Phys. Rev. B 61 (2000) 6401.
[12] J.W. Lynn, B. Keimer, C. Ulrich, C. Bernhard, J.L. Tallon, Phys. Rev. B 61 (2000) 14964.
[13] X.H. Chen, Z. Sun, K.Q. Wang, S.Y. Li, Y.M. Xiong, M. Yu, L.Z. Cao, Phys. Rev. B 63 (2001) 64506.
[14] K. Nakamura, K.T. Park, A.J. Freeman, J.D. Jorgensen, Phys. Rev. B 63 (2001) 24507.
[15] Y. Furukawa, S. Takada, A. Yamanaka, K. Kumagai K, Physica C 341 (2000) 453.
[16] C. Bernhard, J.L. Tallon, E. Brucher, R.K. Kremer, Phys. Rev. B 61 (2000) 14960.
[17] A. Fainstein, P. Etchegoin, H.J. Trodahl, J.L. Tallon, Phys. Rev. B 61 (2000) 15468.
[18] A. Butera, A. Fainstein, E. Winkler, J.L. Tallon, Phys. Rev. B 63 (2001) 54442.
[19] A. Fainstein, E. Winkler, A. Butera, J.L. Tallon, Phys. Rev. B 60 (1999) 12597.
[20] J.D. Jorgensen, O. Chmaissem, H. Shaked, S. Short, P.W. Klamut, B. Dabrowski, J.L. Tallon, Phys. Rev. B 63 (2001) 54440.
[21] R.S. Liu, L.-Y. Jang, H.H. Hung, J.L. Tallon, Phys. Rev. B 63 (2001) 212507.
[22] A.V. Boris, P. Mandal, C. Bernhard, N.N. Kovaleva, K. Pucher, J. Hemberger, A. Loidl, Phys. Rev. B 63 (2001) 184505.
[23] G.V.M. Williams, S. Krämer, Phys. Rev. B 62 (2000) 4132.
[24] I. Felner, U. Asaf, C. Godart, E. Alleno, Physica B 259–261 (1999) 703.
[25] G.V.M. Williams, L.-Y. Jang, R.S. Liu, Phys. Rev. B 65 (2002) 64508.
[26] I. Felner, U. Asaf, E. Galstyan, Phys. Rev. B 66 (2002) 24503.
[27] C.S. Knee, B.D. Rainford, M.T. Weller, J. Mater. Chem. 10 (2000) 2445.
[28] A.C. Mclaughlin, J.P. Attfield, U. Asaf, I. Felner, Phys. Rev. B 68(1) 014503.
[29] I. Dzyaloshinksy, Sov. Phys. JETP 5 (1957) 1259.
[30] T. Moriya, Phys. Rev. 120 (1960) 91.
[31] A.C. Mclaughlin, J.A. McAllister, L.D. Stout, J.P. Attfield, Solid State Sci. 4 (2002) 431.
[32] A.C. Mclaughlin, J.A. McAllister, L.D. Stout, J.P. Attfield, Phys. Rev. B 65 (2002) 172506.
[33] A.C. Mclaughlin, V. Janowitz, J.A. McAllister, J.P. Attfield, Chem. Commun. (2000) 1331.
[34] A.C. Mclaughlin, V. Janowitz, J.A. McAllister, J.P. Attfield, J. Mater. Chem. 11 (2001) 173.
[35] M. Newville, P. Livins, Y. Yacoby, J.J. Rehr, E.A. Stern, Phys. Rev. B 47 (1993) 14126.
[36] A.C. Larson, R.B. Von Dreele, Los Alamos National Report Laboratory Report No. LA-UR-86–748, 1994.
[37] H.M. Rietveld, Acta Crystallogr. 22 (1967) 151.
[38] Z. Hu, H. Von Lips, M.S. Golden, J. Fink, G. Kaindl, F.M.F. de Groot, S. Ebbinghaus, A. Reller, Phys. Rev. B 61 (2000) 5262.